Introduction

Juvenile idiopathic arthritis (JIA) is one of the most common forms of paediatric chronic arthritis, with an incidence of approximately 9.7 per 100 000 children (aged 15 years and under) in Japan [1, 2]. Methotrexate (MTX) is the most common disease-modifying antirheumatic drug used for the treatment of articular-type JIA, namely the polyarticular- and oligoarticular-onset types of JIA [2]. Methotrexate is effective in about 75% of cases of the articular-type JIA, but causes adverse effects, such as liver and/or renal dysfunction [2, 3]. The effects of polymorphisms within the MTX pathway genes on the toxicity and efficacy of MTX in patients with rheumatoid arthritis (RA) and JIA have been studied [4–6].

The influence of polymorphisms within the MTX pathway genes encoding solute carrier family 19 member 1 (SLC19A1), also known as reduced folate carrier (RFC), 5,10-methylenetetrahydrofolate reductase (MTHFR), folypolyglutamate synthetase (FPGS), γ-glutamyl hydrolase (GGH), 5-aminomidazole-4-carboxamide ribonucleotide transformylase (ATIC) and breast cancer resistance protein (BCRP/ABCG2) on the toxicity and efficacy of MTX in patients with RA, JIA and other diseases has been studied [4–9]. However, results regarding the influence of these polymorphisms on the toxicity and efficacy of MTX are conflicting, and there are marked differences in pharmacogenetics between racial groups [10]. Therefore, we investigated whether polymorphisms within the MTX pathway genes were related to the toxicity and efficacy of MTX in 92 patients with articular-type JIA in Japan.

Patients and methods

Study population

Patients were eligible if they met the International League of Association for Rheumatology classification criteria for articular-type JIA [11]. A total of 92 children (74 girls and 18 boys; 12 with seronegative polyarticular onset, 46 with seropositive polyarticular onset and 34 with oligoarticular onset) in this study were treated at the Yokohama City University Hospital between December 2007 and December 2009.

All 92 patients had been treated with MTX for at least 3 months without biologics. Initially, MTX was administered orally at a dosage of 4–5 mg m^{-2} per week. Then the dosage was adjusted depending on tolerability and response (maximal dosage, 10 mg m^{-2} $week^{-1}$) [2]. Prednisolone was used concomitantly with MTX in 89 patients (96.7%). Folic acid supplementation was performed in nine patients (9.9%). Clinical data were collected from a patient's medical record without any knowledge of the individual's polymorphisms.

The study was performed in accordance with the Declaration of Helsinki, and approval for it was obtained from the Yokohama City University School of Medicine Ethics Committee. Each patient or his/her guardians gave written informed consent to participate in this study.

Definitions of toxicity and efficacy

For the evaluation of toxicity, liver dysfunction was defined as an increase in serum alanine transaminase (ALT) level to five times the normal upper limit before the addition of biologics.

Responders to MTX were defined as follows: (i) patients in whom the medication was terminated because they had remission of symptoms; (ii) patients who continued the treatment with stable doses of MTX; and (iii) patients who continued MTX treatment with the concomitant use of acceptable doses of prednisolone, without the addition of biologics, such as anti-tumour necrosis factor therapy [12] and anti-interleukin-6 receptor antibody therapy [13, 14].

Non-responders to MTX were defined as patients who were refractory to MTX and thus treated with biologics. Treatment with biologics was conducted according to the following criteria: (i) patients with a history of treatment with nonsteroidal anti-inflammatory drugs and MTX; and (ii) patients who had the active disease for at least 3 months after MTX treatment (up to 10 mg m^{-2} $week^{-1}$). Active disease was characterized by five or more swollen joints and three or more joints with limited range of movement accompanied by pain and/or tenderness, or the use of high doses of corticosteroids (>0.25 mg kg^{-1} daily), with accompanying unacceptable side-effects [12, 13].

Clinical predictors

Clinical predictors that may influence a patient's disease state and the toxicity and efficacy of MTX were selected on the basis of previous reports [5, 6, 15, 16]. The following factors were included: sex; age at disease onset; duration of MTX treatment; time interval from disease onset to MTX treatment; rheumatoid factor (RF) status; anti-cyclic citrullinated peptide (anti-CCP) status; and concomitant use of prednisolone and folic acid.

Genetic predictors

Genomic DNA was isolated from peripheral blood using the QIAamp DNA Mini kit (Qiagen K.K., Tokyo, Japan).

The following eight single nucleotide polymorphisms (SNPs) within the MTX pathway genes encoding RFC, MTHFR, FPGS, GGH, ATIC and BCRP were selected according to previous reports [4–9]. Genotyping for the SNPs of *RFC* G80A (rs1051266), *MTHFR* A1298C (rs1801131), *MTHFR* C677T (rs1801133), *FPGS* A1994G (rs10106), *GGH* C452T (rs11545078), *GGH* T16C (rs1800909), *ATIC* C347G (rs2372536) and *BCRP* C421A (rs2231142) was performed using the TaqMan assay (Applied Biosystems, Foster City, CA, USA). TaqMan SNP Genotyping Assays were used for *MTHFR* A1298C and *MTHFR* C677T, and Custom TaqMan SNP Genotyping Assays were used for *RFC* G80A, *FPGS*

A1994G, *GGH* C452T, *GGH* T16C, *ATIC* C347G and *BCRP* C421A [9] (see Supplementary data 1). These SNPs were analysed in real-time PCRs by the AB7500 Real Time PCR system (Applied Biosystems), in the conditions recommended by the manufacturer. Allele discrimination was performed using SDS software version 1.4 (Applied Biosystems).

Statistical analysis

For continuous predictors, such as age and duration of MTX treatment, Student's unpaired *t*-test was used to assess the association between clinical predictors and the toxicity and efficacy. For categorical predictors, such as genetic predictors and sex, a χ^2 test and Fisher's exact test were used to assess the association between predictors and the toxicity and efficacy. Possible confounding effects among the predictors were adjusted using a multiple logistic regression model.

Haplotype phases and haplotype frequencies were estimated using the Expectation-Maximization algorithm (minimum haplotype frequency >0.05). All statistical analyses were carried out using the SAS system version 9 (SAS Institute Inc., Cary, NC, USA).

Results

Distribution of the polymorphisms within the MTX pathway genes

The genotype frequencies for the eight SNPs under study were in Hardy–Weinberg equilibrium ($P > 0.05$). Each result was consistent with the findings of a previous report (see Supplementary data 2) [17].

The toxicity of MTX

Of 92 patients, 10 developed liver dysfunction. Methotrexate treatment of longer duration was a risk factor for liver dysfunction (104.3 months with liver dysfunction, 53.6 months without, $P = 0.005$). No other clinical variables were associated with liver dysfunction (Table 1). None of the patients with folic acid supplementation had liver dysfunction. However, this correlation of folic acid supplementation preventing liver dysfunction was not statistically significant, presumably because of the small study population.

Regarding the association between liver dysfunction and genetic predictors, the TT genotype at *GGH* T16C was a low risk factor for liver dysfunction [$P = 0.031$, odds ratio (OR) = 0.20, 95% confidence interval (CI) 0.03–0.98; Table 2 and Supplementary data 3]. In contrast, the non-TT genotype at *GGH* T16C was a high risk factor for liver dysfunction ($P = 0.031$, OR = 5.10, 95% CI 1.02–25.6), which is of significant clinical interest. This association was statistically significant even after adjustment for duration of MTX treatment ($P = 0.028$, OR = 6.90, 95% CI 1.38–34.5). None of the other SNPs was associated with liver dysfunction.

The *MTHFR* haplotypes and *GGH* haplotypes showed no significant associatjon with liver dysfunction (data not shown).

The efficacy of MTX

Of 92 patients, 67 were non-responders to MTX. Delayed MTX treatment from disease onset (21.3 months with non-responders *vs.* 8.5 months with responders, $P = 0.029$) and RF positivity ($P = 0.026$, OR = 2.87, 95% CI 1.11–7.39) were risk factors for lower efficacy of MTX (Table 3). No other clinical variables were associated with efficacy.

Regarding the association between the efficacy of MTX and genetic predictors, there was no gene polymorphism significantly associated with efficacy (Table 4). The *MTHFR* haplotypes and *GGH* haplotypes showed no significant association with efficacy (data not shown).

In 64 patients treated with MTX within 1 year of disease onset, the CC genotype at *ATIC* C347G tended to be associated with lower efficacy. However, this was not statistically significantly after adjustment for the time interval and RF ($P = 0.106$, OR = 0.38, 95% CI 0.12–1.23) (Table 5).

Discussion

Several studies have shown the influence of polymorphisms within the MTX pathway genes on the toxicity and

Table 1

Association between clinical predictors and liver dysfunction

	ALT >5.0 times normal ($n = 10$)	ALT ≤5.0 times normal ($n = 82$)	*P* value
Age at onset (years, mean)	9.5	7.4	0.138
Sex (male)	20.0%	19.5%	0.971
Time interval from onset to treatment (months, mean)	17.7	17.9	0.987
Prednisolone	90.0%	97.6%	0.204
Folic acid	0.0%	11.0%	0.270
Duration of MTX treatment (months, mean)	104.3	52.6	0.005
MTX efficacy	30.0%	26.8%	0.832

ALT, alanine transaminase.

Table 2

Association between genetic predictors and liver dysfunction

Genotype	Allele model* OR†	*P* value	Dominant model* OR†	*P* value	Recessive model* OR†	*P* value
RFC G80A	1.51	0.414	0.21	0.121	0.59	0.627
BCRP C421A	1.05	0.930	0.80	0.840	0.99	0.988
MTHFR C677T	1.45	0.451	1.12	0.896	2.28	0.214
MTHFR A1298C	0.89	0.852	1.08	0.539	0.74	0.655
FPGS A1994G	0.54	0.249	4.88	0.068	0.70	0.600
GGH T16C	0.42	0.118	0.83	0.475	0.20	0.031
GGH C452T	0.61	0.506	–	–	0.61	0.502
ATIC C347G	1.40	0.560	0.48	0.814	1.17	0.336

M, major allele; and m, minor allele. Major alleles are the A allele at *RFC* G80A, C allele at *BRCP* C421A, C allele at *MTHFR* C677T, A allele at *MTHFR* A1298C, G allele at *FPGS* A1994G, T allele at *GGH* T16C, C allele at *GGH* C452T and C allele at *ATIC* C347G. *Allele model: M *vs.* m; dominant model, (MM or Mm) *vs.* mm; recessive model, MM *vs.* (Mm or mm). †Non-adjusted odds ratio.

Table 3

Association between clinical predictors and methotrexate efficacy

	Responder ($n = 25$)	Non-responder ($n = 67$)	*P* value
Age at onset (years, mean)	6.6	7.9	0.180
Sex (male)	12.0%	22.4%	0.264
Time interval from onset to treatment (months, mean)	8.5	21.3	0.029
Prednisolone	96.0%	97.0%	0.807
Folic acid	4.0%	11.9%	0.254
C-reactive protein at start of treatment (mg dl^{-1}, mean)	2.8	3.3	0.685
Anti-cyclic citrullinated peptide [>4.5 (U ml^{-1})]	32.0%	55.2%	0.062
Rheumatoid factor [>14 (IU ml^{-1})]	40.0%	65.7%	0.026

Table 4

Association between genetic predictors and methotrexate efficacy

Genotype	Allele model* OR†	*P* value	Dominant model* OR†	*P* value	Recessive model* OR†	*P* value
RFC G80A	1.01	0.979	1.32	0.572	1.61	0.435
BCRP C421A	1.28	0.496	0.24	0.151	0.99	0.979
MTHFR C677T	0.75	0.399	0.79	0.708	0.42	0.115
MTHFR A1298C	1.05	0.918	0.36	0.282	0.87	0.775
FPGS A1994G	0.95	0.900	1.37	0.726	1.01	0.984
GGH T16C	1.01	0.986	2.83	0.294	1.24	0.654
GGH C452T	1.15	0.805	–	–	1.15	0.805
ATIC C347G	0.65	0.237	1.08	0.931	0.50	0.139

*Allele model: M *vs.* m.; dominant model, (MM or Mm) *vs.* mm; recessive model, MM *vs.* (Mm or mm). †Non-adjusted odds ratio.

efficacy of MTX in patients with RA [4, 8, 9]. However, results are conflicting, and there are marked differences between racial groups in pharmacogenetic studies [10]. We could find only two studies on the pharmacogenetics of MTX in patients with JIA in Caucasian patients [5, 6], but not one in an Asian population. This is the first reported study on pharmacogenetics of MTX in patients with JIA in an Asian population.

First, we found that the non-TT genotype at *GGH* T16C was associated with a high risk of liver dysfunction. This should be taken into consideration in treating patients carrying the non-TT genotype at *GGH* T16C with MTX in order to prevent liver dysfunction.

Once inside the cell, MTX undergoes FPGS-catalysed polyglutamation by the addition of two to seven glutamic acid groups. The polyglutamated form is not

Table 5

Association between *ATIC* 347CC genotype and methotrexate efficacy in patients with the early phase of juvenile idiopathic arthritis

(a)	OR†	95% Confidence interval	*P* value
ATIC 347CC genotype	0.32	0.11–0.93	0.033

(b)	OR‡	95% Confidence interval	*P* value
ATIC 347CC genotype	0.38	0.12–1.23	0.106
Rheumatoid factor [>14 (IU ml^{-1})]	0.22	0.07–0.72	0.012
Time interval*	0.85	0.70–1.04	0.12

*Time interval, time interval from disease onset to methotrexate treatment. †Non-adjusted odds ratio. ‡Adjusted odds ratio.

readily transported across the cell membrane, and thus, the intracellular half-life of MTX is increased. This polyglutamation process is reversed via GGH-catalysed removal of the glutamic acid groups. Therefore, the amount of intracellular MTX-polyglutamates (MTX-PGs) depends on the net rate of polyglutamation determined by the opposing activities of FPGS and GGH [8].

It was reported that *GGH* T16C, which results in a Cys6Arg substitution, was associated with the efficacy of MTX in patients with RA. The variant C allele may cause a loss of GGH activity, resulting in decreased efflux of MTX and thus increased intracellular MTX-PG levels [8]. This result was consistent with ours. Although we did not address the MTX-PG levels in hepatic cells, it is possible that the C allele at *GGH* T16C was associated with reduced GGH activity and thereby increased the MTX-PG levels in hepatic cells. As a result, the risk of liver dysfunction rises. The AA genotype at *FPGS* A1994G tended to be associated with liver dysfunction ($P = 0.068$, OR = 4.88, 95% CI 0.78–30.9). Future research using large study populations to address the effects of the combination of *GGH* and *FPGS* polymorphisms on MTX toxicity is needed.

The MTX dosage was probably associated with the toxicity and efficacy of the drug. In this cohort study, some patients underwent MTX treatment at other hospitals and had liver dysfunction before being referred to our institution. For these patients, we did not have access to previous medical records concerning the exact dosage of MTX at the time of liver dysfunction. As a general rule, non-responders to MTX received higher dosages of MTX (up to 10 mg m^{-2}) before the introduction of biologics than the responders. We therefore used MTX efficacy as the clinical predictor instead of MTX dosage. The MTX efficacy tended to be associated with liver dysfunction ($P = 0.083$), although the effect of MTX dosage on the toxicity and efficacy of this drug should be evaluated directly in the future.

Second, we found that the longer time interval from disease onset to MTX treatment and RF positivity were associated with lower efficacy of MTX. This was consistent with previous research results. Time to treatment was reported as an important factor in the response to MTX in patients with JIA [6], and RF positivity was associated with worse disease activity [18, 19].

Paediatric rheumatologists have recently been able to use MTX for patients with earlier phases of JIA, because MTX has become well known as a first-line drug in the treatment of RA and JIA [2, 3]. Therefore, we analysed the subgroup of early JIA patients. In those who were treated with MTX within 1 year of disease onset, the CC genotype at *ATIC* C347G tended to be associated with the lower efficacy of MTX. Methotrexate-polyglutamates inhibit ATIC, the last enzyme in the *de novo* purine synthesis pathway. Methotrexate achieves part of its anti-inflammatory effect through inhibition of ATIC, which results in the release of the anti-inflammatory agent, adenosine [9].

It was reported that RA patients with the G allele at *ATIC* C347G, resulting in a Thr116Ser substitution, were likely to have a good response to MTX [9]. Although the effect of the C347G polymorphism on ATIC enzyme activity is unknown, *ATIC* C347G may be in linkage disequilibrium with an unknown functional variant, which is associated with the activity of the purine synthesis pathway and with the level of adenosine production. Future basic and clinical prospective studies on a large number of patients are needed to elucidate this association.

There are some limitations to the present study. The incidence of RF positivity in the patient population studied was higher than generally seen (~10%) [18], presumably because our institution is one of the very few paediatric rheumatology centres in Japan, and many severe cases with RF positive are referred to our institution for highly specialized treatment with biologics [13, 20]. The efficacy rate of MTX in this study (28%) was significantly lower than those in previous Japanese reports [2, 3]. This may be due to the use of a new second-line choice of biologics, as well as the characteristics of our institution and the lower limit of the maximal MTX dosage (10 mg m^{-2}) for the treatment of JIA in Japan [2].

In summary, we found an association between the non-TT genotype at *GGH* T16C and liver dysfunction due to MTX. We also found an influence of time interval from disease onset to MTX treatment on the efficacy of MTX in Japanese patients with JIA. Our study showed the importance of early use of MTX for patients with JIA as well as the possibility of more personalized therapy for patients with JIA based on pharmacogenetic study of the MTX pathway genes.

Competing Interests

There are no competing interests to declare.

This work was supported by a grant from Grand-in-Aid for Scientific Research from Japan Society for the Promotion of Science (No. 16790583). We are grateful to Mr C. W. P. Reynolds and Teddy Kamata for their careful linguistic assistance with this manuscript.

REFERENCES

1 Cassidy JT, Petty RE. Juvenile idiopathic arthritis. In: Textbook of Pediatric Rheumatology, 5th edn. eds Cassidy JT, Petty RE. Philadelphia, PA: WB Saunders, 2005; 206–60.

2 Mori M, Naruto T, Imagawa T, Murata T, Takei S, Tomiita M, Itoh Y, Fujikawa S, Yokota S. Methotrexate for the treatment of juvenile idiopathic arthritis: process to approval for JIA indication in Japan. Mod Rheumatol 2009; 19: 1–11.

3 McKendry RJ, Dale P. Adverse effects of low dose methotrexate therapy in rheumatoid arthritis. J Rheumatol 1993; 20: 1850–6.

4 Urano W, Taniguchi A, Yamanaka H, Tanaka E, Nakajima H, Matsuda Y, Akama H, Kitamura Y, Kamatani N. Polymorphisms in the methylenetetrahydrofolate reductase gene were associated with both the efficacy and the toxicity of methotrexate used for the treatment of rheumatoid arthritis, as evidenced by single locus and haplotype analyses. Pharmacogenetics 2002; 12: 183–90.

5 Schmeling H, Biber D, Heins S, Horneff G. Influence of methylenetetrahydrofolate reductase polymorphisms on efficacy and toxicity of methotrexate in patients with juvenile idiopathic arthritis. J Rheumatol 2005; 32: 1832–6.

6 Albers HM, Wessels JA, van der Straaten RJ, Brinkman DM, Suijlekom-Smit LW, Kamphuis SS, Girschick HJ, Wouters C, Schilham MW, le Cessie S, Huizinga TW, Ten Cate R, Guchelaar HJ. Time to treatment as an important factor for the response to methotrexate in juvenile idiopathic arthritis. Arthritis Rheum 2009; 61: 46–51.

7 Laverdière C, Chiasson S, Costea I, Moghrabi A, Krajinovic M. Polymorphism G80A in the reduced folate carrier gene and its relationship to methotrexate plasma levels and outcome of childhood acute lymphoblastic leukemia. Blood 2002; 100: 3832–4.

8 van der Straaten RJ, Wessels JA, de Vries-Bouwstra JK, Goekoop-Ruiterman YP, Allaart CF, Bogaartz J, Tiller M, Huizinga TW, Guchelaar HJ. Exploratory analysis of four polymorphisms in human GGH and FPGS genes and their effect in methotrexate-treated rheumatoid arthritis patients. Pharmacogenomics 2007; 8: 141–50.

9 Dervieux T, Furst D, Lein DO, Capps R, Smith K, Walsh M, Kremer J. Polyglutamation of methotrexate with common polymorphisms in reduced folate carrier, aminoimidazole carboxamide ribonucleotide transformylase, and thymidylate synthase are associated with methotrexate effects in rheumatoid arthritis. Arthritis Rheum 2004; 50: 2766–74.

10 Toffoli G, De Mattia E. Pharmacogenetic relevance of MTHFR polymorphisms. Pharmacogenomics 2008; 9: 1195–206.

11 Petty RE, Southwood TR, Manners P, Baum J, Glass DN, Goldenberg J, He X, Maldonado-Cocco J, Orozco-Alcala J, Prieur AM, Suarez-Almazor ME, Woo P. International League of Associations for Rheumatology. International League of Associations for Rheumatology classification of juvenile idiopathic arthritis: second revision, Edmonton, 2001. J Rheumatol 2004; 31: 390–2.

12 Mori M, Takei S, Imagawa T, Imanaka H, Maeno N, Kurosawa R, Kawano Y, Yokota S. Pharmacokinetics, efficacy, and safety of short-term (12 weeks) etanercept for methotrexate-refractory polyarticular juvenile idiopathic arthritis in Japan. Mod Rheumatol 2005; 15: 397–404.

13 Yokota S, Imagawa T, Mori M, Miyamae T, Aihara Y, Takei S, Iwata N, Umebayashi H, Murata T, Miyoshi M, Tomiita M, Nishimoto N, Kishimoto T. Efficacy and safety of tocilizumab in patients with systemic-onset juvenile idiopathic arthritis: a randomised, double-blind, placebo-controlled, withdrawal phase III trial. Lancet 2008; 371: 998–1006.

14 Nishimoto N, Ito K, Takagi N. Safety and efficacy profiles of tocilizumab monotherapy in Japanese patients with rheumatoid arthritis: meta-analysis of six initial trials and five long-term extensions. Mod Rheumatol 2010; 20: 222–32.

15 Gossec L, Dougados M, Goupille P, Cantagrel A, Sibilia J, Meyer O, Sany J, Daurès JP, Combe B. Prognostic factors for remission in early rheumatoid arthritis: a multiparameter prospective study. Ann Rheum Dis 2004; 63: 675–80.

16 Wessels JA, van der Kooij SM, le Cessie S, Kievit W, Barerra P, Allaart CF, Huizinga TW, Guchelaar HJ. A clinical pharmacogenetic model to predict the efficacy of methotrexate monotherapy in recent-onset rheumatoid arthritis. : Pharmacogenetics Collaborative Research Group. Arthritis Rheum 2007; 56: 1765–75.

17 International HapMap Consortium. The International HapMap Project. Nature 2003; 426: 789–96.

18 Petty RE, Cassidy JT. Polyarthritis. In: Textbook of Pediatric Rheumatology, 5th edn. eds Cassidy JT, Petty RE. Philadelphia, PA: WB Saunders, 2005; 261–73.

19 Adib N, Silman A, Thomson W. Outcome following onset of juvenile idiopathic inflammatory arthritis: II. predictors of outcome in juvenile arthritis. Rheumatology 2005; 44: 1002–7.

20 Yokota S, Mori M, Imagawa T, Murata T, Tomiita M, Itoh Y, Fujikawa S, Takei S. Guidelines on the use of etanercept for juvenile idiopathic arthritis in Japan. Pediatric Rheumatology Association of Japan. Mod Rheumatol 2010; 20: 107–13.

Supporting Information

Additional Supporting Information may be found in the online version of this article:

Supplementary data 1
TaqMan® SNP Genotyping Assays.
Supplementary data 2
Distribustion of gene polymorpshisms under the study.
Supplementary data 3
Distribustion of gene polymorpshisms in patiets with or without liver dysfunction.

Please note: Wiley-Blackwell are not responsible for the content or functionality of any supporting materials supplied by the authors. Any queries (other than missing material) should be directed to the corresponding author for the article.

Research Article

Statistics in Medicine

Received 15 January 2010, Accepted 27 May 2010 Published online 18 April 2011 in Wiley Online Library

(wileyonlinelibrary.com) DOI: 10.1002/sim.3999

Application of the continual reassessment method to a phase I dose-finding trial in Japanese patients: East meets West

Satoshi Morita*†

After cancer-related phase I dose-finding trials are completed in Western countries, further phase I trials are often conducted to determine recommended doses (RDS) for Japanese patients. This may be due to concerns about possible differences in treatment tolerability between Caucasians and Japanese. In most of these, a conventional '3+3' cohort study design is used in making dose escalation decisions, possibly due to its relatively easy implementation. Since its proposal by O'Quigley *et al.* (1990; *Biometrics*, 46:33–48), the continual reassessment method (CRM) has been used increasingly in cancer-related phase I dose-finding studies as an alternative to '3+3' designs. One of the principal advantages of applying a Bayesian CRM may be the utilization of all available prior information to estimate RDS through prior distributions that are assumed for model parameters representing the dose–toxicity relationship. In this paper, we present an application of the Bayesian CRM to a phase I dose-finding study in Japanese patients with advanced breast cancer using an informative prior elicited from clinical investigators. In some settings, it may be appropriate to use an informative prior that reflects the accurate and comprehensive previous knowledge of clinical investigators. On the other hand, for a model-based Bayesian outcome-adaptive clinical trial, it is necessary to establish sufficiently vague priors so that accumulating data dominate decisions as the amount of observed data increases. Thus, we retrospectively investigated the relative strength of the prior using a recently proposed method to compute a prior effective sample size.

Keywords: continual reassessment method; dose-finding; phase I trial; prior distribution; prior effective sample size

1. Introduction

After cancer-related phase I dose-finding trials are completed in Western countries, Japanese investigators often conduct trials using the same regimens in Japan to find the optimal doses for Japanese patients. This may be because of concerns about possible differences in treatment tolerability between Caucasians and Japanese. In many cases, recommended doses (RDs) of treatments have been set at higher levels in Caucasians than in Japanese. For example, a phase I study of Taxotere (docetaxel) monotherapy was undertaken in Caucasians to test dose levels from 5 to 115 mg/m^2 [1]. This study identified 100 mg/m^2 as the RD. A subsequent phase I study in Japan tested dose levels from 20 to 90 mg/m^2, and determined that 60 mg/m^2 was the RD for Japanese patients [2].

Japanese clinical investigators develop phase I trial study designs using observed toxicity data and RD levels identified in Western trials as pre-study information. For example, they test a smaller number of dose levels than the original study at doses that account for the RDs in Caucasian patients. In most of these Japanese phase I trials, a conventional '3+3' cohort design is used for making dose escalation decisions, possibly due to its relatively easy implementation and statistical simplicity and the fact that clinical investigators are in general quite familiar with it.

Since its proposal by O'Quigley *et al.* [3], the continual reassessment method (CRM) has been increasingly used in phase I dose-finding studies in cancer patients as an alternative to the '3+3'

Department of Biostatistics and Epidemiology, Yokohama City University Medical Center, 4-57 Urafune-cho, Minami-ku, Yokohama 232-0024, Japan

**Correspondence to: Satoshi Morita, Department of Biostatistics and Epidemiology, Yokohama City University Medical Center, 4-57 Urafune-cho, Minami-ku, Yokohama 232-0024 Japan.*

†E-mail: smorita@urahp.yokohama-cu.ac.jp

design. The CRM, based on a Bayesian parametric model that includes a logistic and a power model [3, 4] is characterized by one or more model parameters representing the dose–toxicity relationship. Although two-parameter models are flexible, they generally require a larger number of patients to estimate two model parameters, e.g. intercept and slope. One-parameter models that analyze one aspect of the dose–toxicity curve (in many cases, the slope) may not be flexible enough to accurately estimate the entire dose–toxicity curve. However, because a one-parameter model in the CRM has proven to be robust in determining a RD [3], it may be reasonable to use a one-parameter model for dose-finding in a cancer phase I trial.

The prior distributions assumed for model parameters are derived from pre-study information and are updated based on accumulated toxicity data observed in consecutive patient cohorts. The prior distribution of the model parameter should reasonably represent clinical investigators' uncertainty about the dose–toxicity relationship before starting the study, sometimes based on historical data from previous clinical studies. A Bayesian approach that formally uses historical/external data to establish such a prior distribution has not yet been fully developed. However, the integration of any available prior information into the estimation of RD levels for Japanese patients may be one of the major advantages of applying Bayesian CRM.

In some settings, it may be appropriate to use an informative prior that reflects the accurate and comprehensive knowledge that clinical investigators already possess. On the other hand, in other cases one may need to avoid excessively informative priors that may unduly influence posterior inferences. In particular, for clinical trials with a model-based Bayesian outcome-adaptive design, it is necessary to establish sufficiently vague priors so that accumulating data dominate decisions as the amount of observed data increases. After completing a Japanese phase I trial, we were concerned about the strength of the established prior distribution relative to the observed data in the trial in which 16 patients were enrolled in total. Thus, we retrospectively investigated the relative strength of the prior using a recently proposed method to compute a prior effective sample size (ESS) [5]. In this paper, we present an application of the CRM to a phase I dose-finding study in Japanese patients with advanced breast cancer using an informative prior elicited from Japanese clinical investigators.

Section 2 provides a motivating example. In Section 3, we describe the application of the CRM to a Japanese phase I study. We discuss establishment of a prior assumed for a dose–toxicity relationship in Section 4. We close with a discussion in Section 5.

2. A motivating example

Although chemotherapy regimens utilizing infusional 5-FU, e.g. the CEF-infu regimen (cyclophosphamide, epirubicin, and infusional 5-FU) [6], have been shown to have high antitumor activity, such regimens require central venous access and pumps. To avoid these inconveniences, a research team from the European Organization for Research and Treatment of Cancer (EORTC) conducted a phase I dose-finding study to develop a new combination regimen substituting the infusional 5-FU in CEF-infu with capecitabine [7]. Capecitabine (Xeloda®) is a novel oral 5-FU prodrug with high single-agent antitumor activity in metastatic breast cancer [8, 9], and also represents an attractive combination partner for the other CEF-infu chemotherapeutic agents [10–12]. The primary objective of the EORTC study was to determine the RD of capecitabine in combination with epirubicin and cyclophosphamide (CEX) in patients with advanced breast cancer. In the EORTC CEX study, four dose levels were planned for capecitabine in combination with fixed doses of epirubicin and CEX (100 and 600 mg/m^2, day 1, every 3 weeks), as summarized in Table I. Capecitabine was escalated from 750 to 1250 mg/m^2 twice daily for three weeks in four dose levels. A conventional '3+3' cohort design was used when making dose escalation decisions. That is, escalation to the next dose level was permitted if zero out of three (0/3) or one out of six (1/6) patients experienced dose-limiting toxicity (DLT). DLT is usually defined as the occurrence of grade 4 hematologic toxicity and grade 3 or 4 non-hematologic toxicity. If more than one patient developed a DLT, the maximum toxic dose (MTD) was reached, and the previous dose level was defined as the RD for phase II studies. In this study, 11 patients received CEX at four dose levels. While defining the MTD, three, three, three, and two patients were entered at dose levels 1, 2, 3, and 4, respectively, as shown in Table I. No DLTs occurred at dose levels 1, 2, and 3. At dose level 4, two out of two patients experienced DLTs. In addition, a high rate of capecitabine treatment modification (interruption and/or reduction) was required at dose level 3. Thus, the EORTC CEX study concluded

Table I. Dose levels of epirubicin and capecitabine studied in the Japanese and EORTC CEX studies and incidence of dose-limiting toxicities (DLTs) observed in the EORTC CEX study. The dose level of cyclophosphamide was fixed at 600 mg/m^2 on day 1 in both studies.

	Dose level	Epirubicin (mg/m^2, day 1 q21d)	Capecitabine (mg/m^2 twice daily, days 1–14 q21d)	Incidence of DLTs*
Japanese CEX	4	100	900	—
	3	90	900	$\frac{2}{6}$
	2	90	829	$\frac{0}{3}$
	1	75	829	$\frac{1}{4}$
	0	75	628	$\frac{0}{3}$
EORTC CEX	4	100	1250	$\frac{2}{2}$
	3		1050	$\frac{0}{3}$
	2		900	$\frac{0}{3}$
	1		750	$\frac{0}{3}$

*The number of patients experiencing any DLT/the number of evaluable patients.

that the recommended CEX regimen be limited to dose level 2 and consist of capecitabine 900 mg/m^2 twice daily, epirubicin 100 mg/m^2, and CEX 600 mg/m^2.

Although the EORTC study identified a recommended CEX regimen in this way, concern was raised over possible differences in CEX tolerability between Caucasians and Japanese [6, 13]. To answer this question, we conducted a phase I dose-finding trial using the CRM to determine the RDs of the CEX combination in Japanese patients with advanced breast cancer [14, 15]. Based on data from the EORTC CEX study and assuming that the RD of CEX in Japanese patients should not be higher than that in Caucasians, five dose levels (0–4) were planned in the Japanese CEX study, as summarized in Table I. Treatment consisted of a fixed dose of CEX (600 mg/m^2 on day 1) in combination with three doses of epirubicin and three doses of capecitabine. Dose level 4, the highest in our study, corresponded to the CEX RD as determined in the EORTC CEX analysis. The European and Japanese CEX studies employed the same DLT definitions.

3. The CRM in the Japanese cex trial

3.1. Study design using the CRM

3.1.1. Dose–toxicity model. In the CRM we used numerical dose levels X_j for $j=0,\ldots,4$, to reduce the dimension of the dose levels for the CEX treatment consisting of the three anti-cancer agents. The numerical values of X_j were specified using 'backward fitting' [16] as described below, instead of the actual dose levels for the CEX treatment in Table I. This dimension reduction allows a dose–toxicity model to suitably fit the pre-study estimates of the proportion of patients who would experience a DLT at the dose levels. The outcome variable is the indicator $Y_i=1$ if a patient i suffers a DLT, 0 if not. A one-parameter logistic regression model,

$$\pi(X_i,\beta)=\Pr(Y_i=1|X_i,\beta)=\frac{\exp(\beta_0+\beta_1 X_i)}{1+\exp(\beta_0+\beta_1 X_i)} \quad (1)$$

with the intercept b_0 fixed at 3 and a slope parameter b_1, is assumed. The likelihood for n patients is

$$f(\mathbf{Y}_n|\mathbf{X}_n,\beta)=\prod_{i=1}^{n}\pi(X_i,\beta)^{Y_i}\{1-\pi(X_i,\beta)\}^{1-Y_i}. \quad (2)$$

3.1.2. Setting up the CRM. Before starting the study, we conducted a preliminary study among participating clinical oncologists to obtain necessary reference information for implementing the CRM. We set up the CRM design using the following five steps:

(i) In step 1, we identified the target DLT probability as 0.33 and obtained the prior estimates of the proportion of patients who would experience a DLT at each dose level from 0 to 4 as 0.05, 0.10, 0.25, 0.40, and 0.60, respectively.

(ii) In step 2, we predetermined the model's intercept b_0 at 3, as discussed in Section 3.1.3.
(iii) In step 3, we specified a prior distribution function of the slope b_1. Letting $Ga(a,b)$ denote the gamma distribution with mean a/b and variance a/b^2, we assumed $Ga(a,b)$ for b_1 in order to constrain the slope b_1 to be positive and for computational convenience. This constraint implies an assumption that a higher dose level increases the probability of DLT.
(iv) In step 4, we specified numerical values of X_j for $j=0,\ldots,4$ using backward fitting as follows. We added a constraint $E(b_1)=1$ that corresponds to an equation $a=b$ in the gamma prior distribution to make the *a priori* dose–toxicity curve exactly reflect the prior estimate of DLT occurrence probabilities regardless of the degree of clinical uncertainty [17]. Under the dose–toxicity model with the slope b_1 fixed at 1, we computed each X_j to match $\Pr(Y=1|X_j,\beta_0=3,\beta_1=1)$ with the prior probability estimate of DLT occurrence at dose level j for $j=0,\ldots,4$. As a result, $\{X_0,X_1,X_2,X_3,X_4\}=\{-5.94,-5.20,-4.10,-3.41,-2.60\}$.
(v) In step 5, we specified the hyperparameters of the prior $p(b_1|a,b)$ as $a=b=5$. Details of this step are described in Section 4.

3.1.3. Specification of the intercept b_0. Under $a=b=5$ and $b_0=3$, the prior dose-toxicity curve with a 90 per cent credible interval is given in Figure 1(a). This prior dose-toxicity curve may reflect the oncologist's greater confidence in higher rather than lower dose levels. That is, taking into account that dose level 4 in the Japanese CEX study corresponds to the RD identified in the EORTC CEX study, $b_0=3$ may be a reasonable choice. In contrast, if we use a negative value for the intercept, i.e. $b_0=-5$, $\{X_0,X_1,X_2,X_3,X_4\}$ is computed as $\{2.06, 2.80, 3.90, 4.59, 5.41\}$ using backward fitting. In this setting, the prior dose–toxicity curve represents greater uncertainty in higher rather than lower dose levels (Figure 1(b)) and therefore should be considered that the specification $b_0=-5$ contradicts the pre-study information.

3.1.4. Dose escalation/de-escalation rule. Our study plan involved treating up to 22 patients. The starting dose was level 1, which was given to the first enrolled patient. The CRM then ran sequentially with three patients per cohort. Each cohort was treated at the dose level X_j with an estimated probability of DLT $\pi\{X_j,E(\beta_1|\text{data})\}$ closest to 0.33 and not exceeding 0.40. If the computed probability of the suggested dose level was greater than 0.40, the cohort was treated at the preceding dose level. Untried doses were not skipped when escalating dose level. The trial was stopped if level 0 was considered too toxic to be administered, e.g. $\pi\{X_0,E(\beta_1|\text{data})\}>0.40$. The posterior distribution of the slope parameter b_1 and each posterior estimate $\pi\{X_j,E(\beta_1|\text{data})\}$ along with its 90 per cent credible

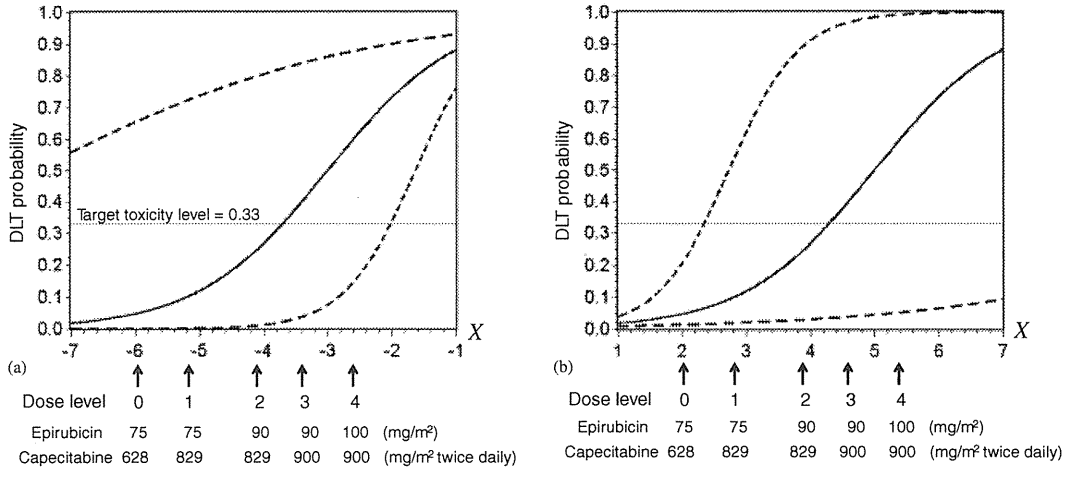

Figure 1. (a) Prior dose–toxicity curve (solid line) and its 90 per cent credible intervals (dashed lines) with the intercept $b_0=3$ under the gamma prior distribution, Ga (5,5). The horizontal axis X denotes the dose levels. The five values of $\{X1, X2, X3, X4, X5\}=\{-5.94,-5.20,-4.10,-3.41,-2.60\}$ used in the CRM computation are indicated by arrows. *The actual dose levels of epirubicin and capecitabine are also shown.* The horizontal straight line indicates the target DLT level (0.33) and (b) Prior dose–toxicity curve and its 90 per cent credible intervals with the intercept $b_0=-3$.

Table II. Incidence of dose-limiting toxicities (DLTs).

	Cohort 1	Cohort 2	Cohort 3	Cohort 4	Cohort 5	Cohort 6
No. of evaluable patients	1	3	3	3	3	3
Doselevel*	1	0	1	2	3	3
Epirubicin (mg/m^2, day 1 q21d)	75	75	75	90	90	90
Capecitabine (mg/m^2 twice daily, days 1–14 q21d)	829	628	829	829	900	900
No. of patients experiencing any DLT	1	0	0	0	1	1
Grade 3 HFS†	1	—	—	—	—	—
Grade 3 anorexia	—	—	—	—	1	—
Grade 3 mucositis	—	—	—	—	—	1

*The dose level of CEX was fixed at 600 mg/m^2 on day 1 every 3 weeks.
†HFS, hand-foot syndrome.

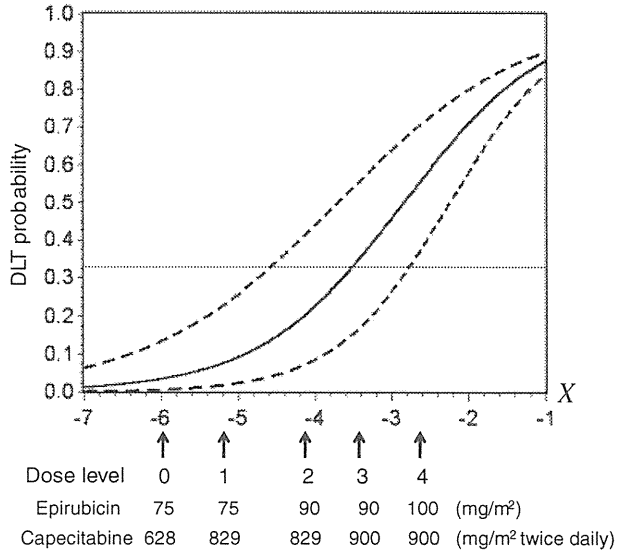

Figure 2. The posterior mean dose–toxicity curve (solid line) and its 90 per cent credible intervals (dashed lines) after updating with the toxicity data from all 16 patients.

interval were computed using numerical integration. An Independent Data and Safety Monitoring Committee (IDSMC) reviewed the interim analyses and was assigned the responsibility of making any recommendations to stop the trial on both clinical and statistical perspectives.

3.2. Implementation of the CRM

Because the results of the Japanese CEX trial were reported in detail in Saji *et al.* [14] and Morita *et al.* [15], we report here in brief. DLTs observed at each dose level and the dose escalation/de-escalation history throughout the study are shown in Tables I and II, respectively. The first patient treated at level 1 experienced a DLT (grade 3 hand-foot syndrome). The dose level was then de-escalated to level 0 for the second cohort. No DLTs were identified in the second, third (level 1), and fourth (level 2) cohorts. One of three patients in cohort 5 treated at level 3 experienced DLT (grade 3 anorexia). In the next cohort treated at level 3, one patient experienced DLT (grade 3 mucositis). Figure 2 shows the updated dose–toxicity curve including toxicity data from these 16 patients. The estimated DLT occurrence probability at level 3 was 0.354 (90 per cent credible interval: 0.174–0.560). With respect to efficacy data, one complete response and three partial responses were observed in six patients at level 3. Taking these CRM computations and the encouraging efficacy data into account, the DSMC recommended that the study be stopped. Therefore, we terminated the study and recommended that dose level 3 be further evaluated in a phase II trial.

4. Establishing a prior

In clinical trials with Bayesian model-based study designs, the prior should reasonably represent the physician's uncertainty. We established the prior distribution used in the Japanese CEX study based on the knowledge and experience of the participating clinical oncologists with regards to the CEX regimen. As described in Section 3, we assumed a gamma distribution Ga(a, b) for the prior distribution of the slope parameter b_1. Subject to $a=b$, the hyperparameter a determines the credible interval of the prior dose–toxicity curve under the gamma prior Ga(a, b). Thus, we determined that the hyperparameter a appropriately depicted the pre-study perceptions of the surveyed oncologists regarding the dose–toxicity relationship. By adjusting the hyperparameter a, i.e. $a=2$, 8, 20, 40, in addition to $a=5$ (Figure 1(a)) we created several graphical presentation patterns as shown in Figure 3. The clinical oncologists consulted in this study came to the consensus that the DLT probability at dose level 1 would be unlikely to be higher than 0.7 (more than double the target DLT level of 0.33) and the DLT probability at dose level 4 would be at least higher than 0.15 (around half of the target DLT level). The oncologists also concurred that the prior dose–toxicity curve and its credible interval constructed at $a=5$ reasonably reflected their knowledge and contained a sufficiently large degree of clinical uncertainty.

Although we determined the hyperparameters of the prior of b_1 based on an extensive discussion of the previous data using meticulous graphical presentations, our choice of the hyperparameters was arbitrary. If an established prior is overly informative, the prior may unduly influence posterior inferences and decisions, particularly early in the trial. Since dose levels must be selected sequentially in phase I dose-finding trials based on very small amounts of data, it may be important to quantify information contained in the chosen priors. These concerns may be addressed by quantifying the prior information

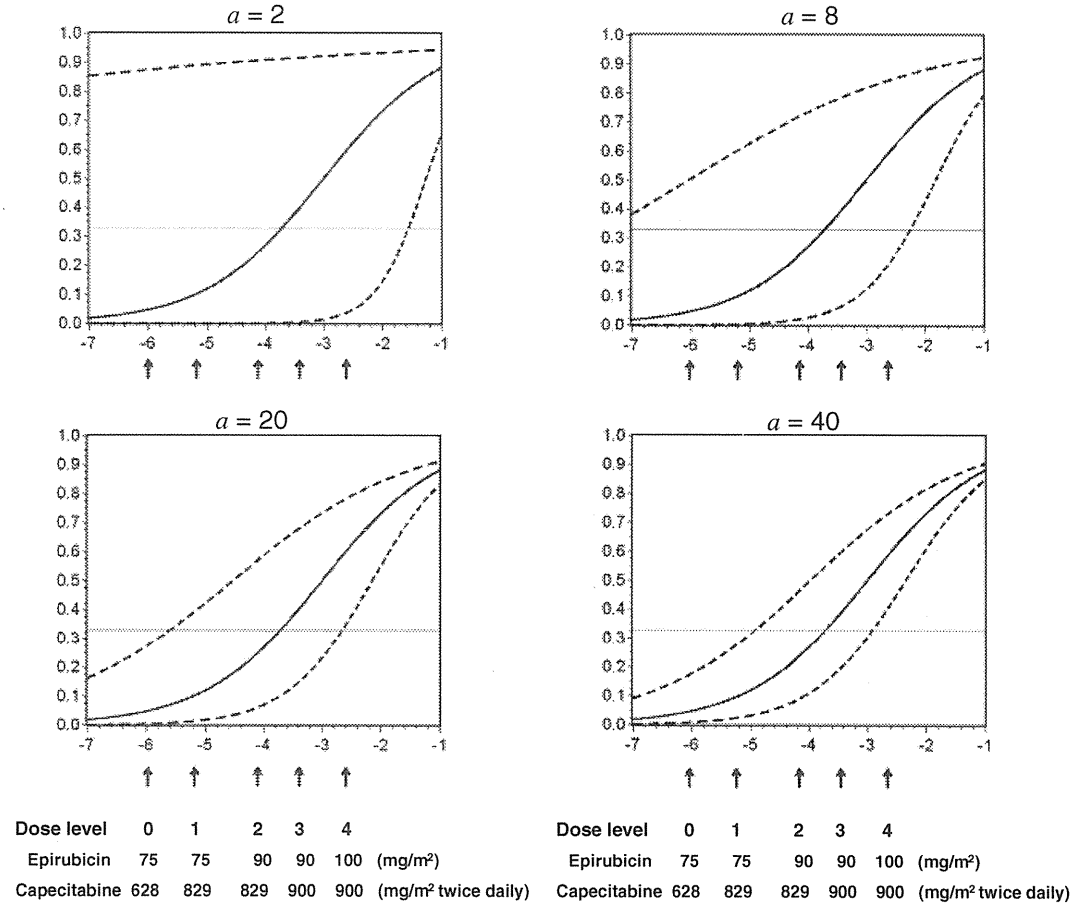

Figure 3. *Prior dose–toxicity curves with hyperparameters a=2, 8, 20, and 40.* Dashed lines indicate its 90 per cent credible intervals.

in terms of an equivalent number of hypothetical patients, i.e. a prior ESS. Such a summary would allow one to judge the relative contributions of the prior and the data to the decisions. We applied an ESS method proposed recently by Morita *et al.* [5] to the Japanese CEX trial in a retrospective fashion. The prior ESS computed at $a=5$ was 2.1. Thus, after enrolling three patients, the information from the likelihood started to dominate the prior, as desired. In addition, under Ga(5,5), the coefficient of variation (=standard deviation/mean) of the slope parameter b_1 was approximately 0.45, which might indicate some uncertainty in the slope parameter. Hence the prior specified in the Japanese CEX trial seemed quite reasonable.

As for the sensitivity analysis of the prior, the prior ESS values computed at $a=2$, 6, 7, 8, 20, and 40 are 0.86, 2.6, 3.0, 3.4, 8.6, and 17.1, respectively. It appears that $a<7$ may be needed to ensure an ESS<3. The prior with $a=40$ has ESS$=17.1$, so that it has impact roughly equal to that of the data on the posterior inference, as suggested by comparing Figures 2 and 3. In addition, under $a=40$, the *a priori* 90 per cent credible interval for the increase in the odds of a DLT occurrence, e.g. for the dose escalation from level 1 to level 2, is computed as 2.3–4.1, which may be excessively narrow compared with the 90 per cent credible interval of 1.5–7.5 computed under $a=5$. Thus, given the limited amount of information available during the design stage of the Japanese CEX study, the prior with $a=40$ may be criticized as being overly informative.

5. Discussion

When designing a phase I dose-finding study using a Bayesian CRM, certain choices must be made regarding details involved in a dose–toxicity model, numerical values of dose levels, prior distributions of model parameters, etc., and these should be sensible and plausible. If a one-parameter logistic model is chosen for modeling a dose–toxicity relationship, as was our approach in the Japanese CEX study, the intercept has to be specified at a certain real value. The actual dose levels of the combination therapy planned in the Japanese CEX study were based on information from the identical regimen conducted earlier in Caucasian patients, the EORTC CEX trial. In order to reduce the dimension of the dose levels, we specified the numerical values of the dose levels in the dose–toxicity formulation using backward fitting. In addition, we established the prior distribution of the slope parameter in the Japanese phase I trial by eliciting pre-study perceptions regarding the dose–toxicity relationship from Japanese clinical investigators.

So far, in many cases Japanese clinical investigators have conducted phase I studies assuming that a RD in Japanese patients should be lower than in Caucasian patients, based on results of clinical trials conducted in Western countries. That is, a large amount of historical data based on numerous studies has been integrated to design Japanese phase I trials. The Japanese CEX study, however, did not take full advantage of the pre-study information on dose–toxicity relationships derived from the EORTC CEX study to formally establish the prior distribution of the model parameter in the CRM.

Differences in RDs may be caused by specific differences between the abilities of Japanese and Caucasian populations to tolerate particular toxicities. These interracial differences can be regarded as patient prognostic covariates, but unfortunately such covariates have not yet been identified. Extensions of methods to find RDs for ordered prognostic subgroups have been proposed by O'Quigley and Paoletti [18], Yuan and Chappell [19], and Ivanova and Wang [20]. These methods may be applied to identifying RDs within racial subgroups in the setting of a multinational phase I study. Thall *et al.* [21] have proposed a Bayesian sequential phase I/II dose-finding design accounting for patient covariates and dose–covariate interactions. This method may also prove useful in modeling the Japanese–Caucasian association in a multinational study setting. It may be a significant challenge, however, to construct informative prior(s) on such an interracial difference in dose–toxicity curves [22].

In the context of Bayesian clinical trial design, well-chosen priors are important to ensure that posterior-based decision rules have good study operating characteristics. Some appropriate criteria for calibrating priors may be desired to obtain sensible prior distributions. A prior ESS quantifying the prior information in terms of the number of hypothetical patients may provide a useful tool for understanding the impact of prior-related assumptions. A useful property of prior ESS is that it is readily interpretable by clinical investigators who are involved in designing a clinical trial. ESS_RegressionCalculator.R, a computer program used to calculate the ESS for a normal linear or logistic regression model, is available from the website http://biostatistics.mdanderson.org/SoftwareDownload.

Acknowledgements

Satoshi Morita's research was supported in part by Grant H20-CLINRES-G-009 from the Ministry of Health, Labour and Welfare of Japan. He is grateful to Dr Masakazu Toi and Dr Junichi Sakamoto for providing important advice and suggestions. The author thanks the associate editor and the two referees for their constructive and helpful comments and suggestions.

References

1. Extra JM, Rousseau F, Bruno R, Clavel M, Le Bail N, Marty M. Phase I and pharmacokinetic study of taxotere (RP 56976; NSC 628503) given as a short intravenous infusion. *Cancer Research* 1993; **53**:1037–1042.
2. Taguchi T, Furue H, Niitani H, Ishitani K, Kanamaru R, Hasegawa K, Ariyoshi Y, Noda K, Furuse K, Fukuoka M, Yakushiji M, Kashimura M. Phase I clinical trial of RP 56976 (docetaxel) a new anticancer drug. *Japanese Journal of Cancer and Chemotherapy* (*Gan To Kagaku Ryoho*) 1994; **21**:1997–2005 (in Japanese).
3. O'Quigley J, Pepe M, Fisher L. Continual reassessment method: a practical design for phase I clinical trials in cancer. *Biometrics* 1990; **46**:33–48.
4. O'Quigley J, Shen LZ. Continual reassessment method: a likelihood approach. *Biometrics* 1996; **52**:673–684.
5. Morita S, Thall PF, Müller P. Determining the effective sample size of a parametric prior. *Biometrics* 2008; **64**:595–602.
6. Bonnefoi H, Biganzoli L, Cufer T, Mauriac L, Hamilton A, Schaefer P, Piccart M. An EORTC phase I study of epirubicin in combination with fixed doses of cyclophosphamide and infusional 5-fu (CEF-infu) as primary treatment of large operable or locally advanced/inflammatory breast cancer. *Breast Cancer Research and Treatment* 2001; **70**:55–63.
7. Bonnefoi H, Biganzoli L, Mauriac L, Cufer T, Schaefer P, Atalay G, Piccart M. An EORTC phase I study of capecitabine (Xeloda) in combination with fixed doses of cyclophosphamide and epirubicin (CEX) as primary treatment for large operable or locally advanced/inflammatory breast cancer. *European Journal of Cancer* 2003; **39**:277–283.
8. Blum JL, Jones SE, Buzdar AU, Lo Russo PM, Kuter I, Vogel C, Osterwalder B, Burger HU, Brown CS, Griffin T. Multicenter phase II study of capecitabine in paclitaxel-refractory metastatic breast cancer. *Journal of Clinical Oncology* 1999; **17**:485–493.
9. Blum JL, Dieras V, Lo Russo PM, Horton J, Rutman O, Buzdar A, Osterwalder B. Multicenter, phase II study of capecitabine in taxane-pretreated metastatic breast carcinoma patients. *Cancer* 2001; **92**:1759–1768.
10. O'Shaughnessy J, Miles D, Vukelja S, Moiseyenko V, Ayoub JP, Cervantes G, Fumoleau P, Jones S, Lui WY, Mauriac L, Twelves C, Van Hazel G, Verma S, Leonard R. Superior survival with capecitabine plus docetaxel combination therapy in anthracycline-pretreated patients with advanced breast cancer: phase III trial results. *Journal of Clinical Oncology* 2002; **20**:2812–2823.
11. Blum JL, Dees EC, Chacko A, Doane L, Ethirajan S, Hopkins J, McMahon R, Merten S, Negron A, Neubauer M, Ilegbodu D, Boehm KA, Asmar L, O'Shaughnessy JA. Phase II trial of capecitabine and weekly paclitaxel as first-line therapy for metastatic breast cancer. *Journal of Clinical Oncology* 2006; **24**:4384–4390.
12. Gradishar WJ, Meza LA, Amin B, Samid D, Hill T, Chen M. Capecitabine plus paclitaxel as front-line combination therapy for metastatic breast cancer: a multicenter phase II study. *Journal of Clinical Oncology* 2004; **22**:2321–2327.
13. Iwata H, Nakamura S, Toi M, Shin E, Masuda N, Ohno S, Takatsuka Y, Hisamatsu K, Yamazaki K, Kusama M, Kaise H, Sato Y, Kuroi K, Akiyama F, Tsuda H, Kurosumi M. Interim analysis of a phase II trial of cyclophosphamide, epirubicin and 5-fluorouracil (CEF) followed by docetaxel as preoperative chemotherapy for early stage breast carcinoma. *Breast Cancer* 2005; **12**:99–103.
14. Saji S, Toi M, Morita S, Iwata H, Ito Y, Ohno S, Kobayashi T, Hozumi Y, Sakamoto J. Dose-finding phase I and pharmacokinetic study of capecitabine (xeloda) in combination with epirubicin and cyclophosphamide (CEX) in patients with inoperable or metastatic breast cancer. *Oncology* 2007; **72**:330–337.
15. Morita S, Toi M, Saji S, Iwata H, Ohno S, Ito Y, Kobayashi T, Hozumi Y, Sakamoto J. Practical application of the continual reassessment method to a phase I dose-finding trial in advanced breast cancer. *Drug Information Journal* 2007; **41**:691–700.
16. Garrett-Mayer E. The continual reassessment method for dose-finding studies: a tutorial. *Clinical Trials* 2006; **3**:57–71.
17. Ishizuka N, Morita S. Practical implementation of the continual reassessment method. In *Handbook of Statistics in Clinical Oncology* (2nd edn), Crowley J (ed.). CRC Press: New York, 2005; 97–116.
18. O'Quigley J, Paoletti X. *Continual reassessment method for ordered groups. Biometrics* 2003; **59**:430–440.
19. Yuan Z, Chappell R. Isotonic designs for phase I cancer clinical trials with multiple risk groups. *Clinical Trials* 2004; **1**:499–508.
20. Ivanova A, Wang K. Bivariate isotonic design for dose-finding with ordered groups. *Statistics in Medicine* 2006; **25**:2018–2026.
21. Thall PF, Nguyen HQ, Estey EH. Patient-specific dose finding based on bivariate outcomes and covariates. *Biometrics* 2008; **64**:1126–1136.
22. Garthwaite PH, Kadane JB, O'Hagan A. Statistical methods for eliciting probability distributions. *Journal of the American Statistical Association* 2005; **100**:680–701.

JOURNAL OF INTERFERON & CYTOKINE RESEARCH
Volume 31, Number 7, 2011

DOI: 10.1089/jir.2010.0142

Placental Growth Factor and Soluble c-Kit Receptor Dynamics Characterize the Cytokine Signature of Imatinib in Prostate Cancer and Bone Metastases

Paul Mathew,[1,*] Sijin Wen,[2] Satoshi Morita,[3] and Peter F. Thall[2]

To assess the hypothesis that the dynamics of plasma angiogenic and inflammatory cytokines after docetaxel chemotherapy with or without the c-kit/abl/platelet-derived growth factor receptor (PDGFR) inhibitor imatinib mesylate for prostate cancer are associated with outcome, the kinetics of 17 plasma cytokines before versus after chemotherapy were assessed and associations with progression-free survival (PFS) examined. After adjusting for multiple tests, significantly different declines in placental growth factor (PIGF), soluble vascular endothelial growth factor receptor-1 (VEGFR1), VEGF, and soluble c-kit were observed with docetaxel plus imatinib ($n = 41$) compared to docetaxel alone ($n = 47$). Based on a piecewise linear regression model for change in concentration of each cytokine as a function of the probability of change in p-PDGFR *in vivo*, only the dynamics of PIGF ($P < 0.0001$) and soluble c-kit ($P < 0.0001$) differed with imatinib therapy. In a Bayesian log-normal regression model for PFS, a rise in human matrix metalloproteinase 9 after docetaxel alone associated with a longer PFS. Distinct plasma angiogenic cytokines are modified by imatinib and partitioned by *in vivo* p-PDGFR dynamics after docetaxel chemotherapy for metastatic prostate cancer. Plasma PIGF and soluble c-kit kinetics are candidate biomarkers of imatinib effect. The predictive value of human matrix metalloproteinase 9 kinetics for docetaxel efficacy requires prospective validation.

Introduction

Improved outcomes with docetaxel chemotherapy for advanced castration-resistant prostate cancer are being sought with novel combinations that target putative mechanisms of disease progression and drug resistance. Preclinical modeling indicated that the platelet-derived growth factor and its receptor (PDGFR) were upregulated in prostate cancer cells proliferating within the bone microenvironment (Uehara and others 2003). The PDGFR was observed to be upregulated in endothelial cells of vasculature specifically associated with PDGF-expressing tumor, and the PDGFR inhibitor imatinib potentiated taxane efficacy via enhanced endothelial apoptosis, an antivascular effect (Uehara and others 2003; Kim and others 2006).

Contrary to preclinical estimates, a randomized controlled study that compared the efficacy of imatinib in combination with docetaxel versus docetaxel alone in men with castration-resistant prostate cancer and bone metastases showed no added benefit with imatinib (Mathew and others 2007). Unexpectedly, *in vivo* pharmacodynamic monitoring of PDGFR inhibition showed that, within the docetaxel arm, an increased probability of PDGFR activation in peripheral blood leucocytes correlated with improved progression-free survival (PFS) and overall survival (OS) (Mathew and others 2008). Rising plasma PDGF levels were associated with a decreased probability of PDGFR activation and inferior PFS (Mathew and others 2008). While the fundamental biological implications of these observations are yet to be determined, these partitioned outcomes were not equally detected in the docetaxel–imatinib combination arm.

To further explore the dynamic signature of plasma cytokines and their prognostic impact after docetaxel chemotherapy, a panel of 17 additional angiogenic and inflammatory cytokines was constructed. Individual cytokine kinetics between baseline (BL) and after docetaxel exposure, modulation by concurrent PDGF inhibitor therapy, and association with PFS outcomes were studied.

Methods

Patients

One hundred sixteen men were enrolled to a randomized study of docetaxel with placebo or imatinib for metastatic castration-resistant prostate cancer and bone metastases (Mathew and others 2007). Of these, 88 paired plasma samples

Departments of [1]Genitourinary Medical Oncology and [2]Biostatistics, University of Texas M.D. Anderson Cancer Center, Houston, Texas.
[3]Department of Biostatistics and Epidemiology, Yokahama City University Medical Center, Yokahama, Japan.
*Present address: Department of Hematology–Oncology, Tufts Medical Center, Boston, Massachusetts.

at BL and 6 weeks later after one cycle of weekly docetaxel-based therapy at cycle 2 day 1 (C2D1) were available.

Multiplex cytokine assay

Plasma levels of all analytes described here were subsequently analyzed in duplicates using a multiplex platform, Meso Scale Discovery (MSD) (Gaithersburg, MD). The analytes were soluble c-kit receptor (c-kit), soluble vascular endothelial growth factor receptor-2 (sVEGFR2, KDR), fibroblast growth factor, VEGF, sVEGFR1, placental growth factor (PIGF), interleukin (IL)2, IL8, IL12p70, IL10, granulocyte macrophage-colony stimulating factor, interferon-γ, IL6, IL10, tumor necrosis factor-α, transforming growth factor-β, and matrix metalloproteinase-(MMP)-9. All reagents were provided with the MSD kits and tests conducted according to the manufacturer's instructions.

Statistical methods

Numerical variables were summarized using means and standard deviations, with association between pairs of variables estimated by Pearson's correlation coefficient (Snedecor and Cochran 1980). The Wilcoxon signed rank test was used for 2 sample comparisons of numerical variables (Hollander and Wolfe 1979), applying the Bonferroni P value correction for multiple tests (Snedecor and Cochran 1980). For each cytokine, the Bayesian regression model and method of Morita and others (2010) were employed to evaluate the effects of change in the cytokine level from BL to C2D1 on PFS time while accounting for the effects of hemoglobin, change in prostate-specific antigen (PSA), and change in p-PDGFR. For each patient, because p-PDGFR was measured in ~2,000 cells both at BL and at C2D1, the within-patient BL and C2D1 distributions of p-PDGFR could be estimated very reliably. Because both the BL and C2D1 distributions of p-PDGFR were clearly bimodal for all patients, the within-patient change in p-PDGFR could not be summarized usefully as the difference between the C2D1 and BL sample means. Rather, a mixture model accounting for the observed bimodality first was fit and used to estimate the differences between the right modes, denoted by δ_{Ri}, and the differences between the left modes, denoted by δ_{Li}, for the within-patient C2D1-versus-BL distributions of p-PDGFR, for each patient, $i = 1, \ldots, 88$.

In the Bayesian regression model for PFS (Morita and others 2010), δ_{Ri} was used as a covariate representing change in p-PDGFR from BL to C2D1. This was done because the values of δ_{Ri} were much larger than δ_{Li}, and moreover δ_{Ri} was strongly associated with longer PFS. Based on preliminary goodness-of-fit analyses, it was assumed that the logarithm of PFS time was normally distributed, equivalently, that PFS was lognormal. The linear component of the lognormal regression model is the mean of log(PFS time), defined as follows. For patient i and cytokine $j = 1, \ldots, 17$, denote the (BL, C2D1) cytokine values by (X_{ij}, Y_{ij}), the difference between the log-transformed cytokine values by $W_{ij} = \log(Y_{ij}) - \log(X_{ij})$, $Z_{1i} = 1$ if treatment was docetaxel+imatinib (DI) and 0 if docetaxel+placebo (DP), $Z_{2i} =$ Hb at BL, and $Z_{3i} =$ change in PSA from BL to C2D1. For cytokine j and patient i, the linear component was assumed to be

$$\begin{aligned}\eta_j = {} & \beta_0 + \beta_1 Z_{1i} + \{\beta_2 Z_{1i} + \beta_3(1 - Z_{1i})\} Z_{2i} \\ & + \{\beta_4 Z_{1i} + \beta_5(1 - Z_{1i})\} Z_{3i} \\ & + \{\beta_6 Z_{1i} + \beta_7(1 - Z_{1i})\} \delta_{Ri} \\ & + \{\beta_8 Z_{1i} + \beta_9(1 - Z_{1i})\} W_{ij}\end{aligned}$$

In terms of their effects on PFS time, the parameters in the linear term may be interpreted as follows:

β_1 = main DI-vs-DP treatment effect
β_2 = effect of baseline Hb in the DI arm
β_3 = effect of baseline Hb in the DP arm
β_4 = effect of change in PSA in the DI arm
β_5 = effect of change in PSA in the DP arm
β_6 = effect of change in p-PDGFR in the DI arm
β_7 = effect of change in p-PDGFR in the DP arm
β_8 = effect of change in cytokine value in the DI arm
β_9 = effect of change in cytokine value in the DP arm

Using the large ($n = \sim 2{,}000$ cells) within-patient p-PDGFR samples taken at BL and at C2D1, the probability of decrease in p-PDGFR after treatment, denoted by Pr(Decr), was estimated very reliably for each patient as a standardized Wilcoxon statistic. Specifically, each patient's Pr(Decr) was computed as the mean over all 0/1 indictors that each BL value of p-PDGFR was larger than each C2D1 value. For each cytokine, the following piecewise linear regression model for the BL to C2D1 change in cytokine value, W_{ij}, as a function of the estimated Pr(Decr) was fit.

$$\begin{aligned}W_{ij} &= b_{0,t} + e_{ij} \text{ if } \Pr(\text{Decr}) \le 0.5 \\ &= b_{0,t} + b_{1,t} * \{\Pr(\text{Decr}) - 0.5\} \\ &\quad + e_{ij} \text{ if } \Pr(\text{Decr}) > 0.5,\end{aligned}$$

for treatment arm $t =$ DI or DP, where e_{ij} denotes normally distributed random measurement error. Under this model, in treatment arm t, on average the BL to C2D1 change in the cytokine value equals the constant $b_{0,t}$ if Pr(Decr) $\le$0.5 and equals the straight line $b_{0,t} + b_{1,t}$ *{Pr(Decr) – 0.5} if Pr(Decr) > 0.5. The cut-off 0.5 was used because Pr(Decr) = 0.5 corresponds to no change in the cytokine from BL to C2D1, whereas Pr(Decr) $\ge$ 0.5 and Pr(Decr) < 0.5 correspond, respectively, to the cytokine going down or up, on average. The piecewise linear form was chosen based on preliminary goodness-of-fit plots of each cytokine change as a function of Pr(Decr). Under the null hypothesis $(b_{0,DP}, b_{1,DP}) = (b_{0,DI}, b_{1,DI})$, the piecewise linear model is the same for the 2 treatment arms. This null hypothesis corresponds to the kinetics of the cytokine, as a function of Pr(Decr), not changing with the addition of imatinib to docetaxel.

Results

The distributions of the 17 plasma angiogenic and inflammatory cytokines at BL and at C2D1 within each treatment arm are summarized in Table 1. These results indicate a significant decline in IL6 and significant increases in PIGF and soluble VEGFR1 in the docetaxel-placebo arm, and a significant decline in soluble c-kit and increase in IL10 in the docetaxel-imatinib arm. Table 2 summarizes changes in cytokine values from BL to C2D1, compared between treatment arms using the Wilcoxon rank sum test. These tests indicate significantly larger declines in PIGF, soluble c-kit,

TABLE 1. MEANS AND STANDARD DEVIATIONS (IN PARENTHESES) OF CYTOKINE VALUES AT BASELINE AND AT COURSE 2 DAY 1 OF CHEMOTHERAPY

	Docetaxel + placebo			*Docetaxel + imatinib*		
Cytokines	*BL*	*C2D1*	*P*	*BL*	*C2D1*	*P*
TGFβ	0.84 (0.22)	0.90 (0.19)	0.009	0.82 (0.22)	0.79 (0.18)	0.586
bFGF	−1.67 (0.24)	−1.67 (0.24)	0.439	−1.65 (0.22)	−1.64 (0.21)	0.881
PIGF	−1.30 (0.09)	−1.20 (0.12)	<0.001[a]	−1.28 (0.09)	−1.35 (0.11)	0.002
sVEGFR1	−0.68 (0.08)	−0.60 (0.10)	<0.001[a]	−0.65 (0.14)	−0.61 (0.26)	0.166
VEGF	−0.77 (0.14)	−0.73 (0.17)	0.05	−0.80 (0.17)	−0.86 (0.16)	0.004
c-kit	0.85 (0.16)	0.86 (0.15)	0.508	0.83 (0.13)	0.70 (0.15)	<0.001[a]
sVEGFR2	1.23 (0.13)	1.24 (0.14)	0.317	1.21 (0.15)	1.19 (0.15)	0.021
hMMP9	1.95 (0.22)	1.99 (0.29)	0.354	1.91 (0.25)	1.83 (0.23)	0.074
GM-CSF	−0.64 (1.14)	−0.68 (1.10)	0.529	−0.47 (0.71)	−0.58 (0.80)	0.05
IFNγ	−0.02 (0.74)	−0.20 (0.77)	0.071	0.13 (0.67)	0.09 (0.89)	0.834
IL10	0.39 (0.92)	0.56 (0.79)	0.019	0.64 (0.67)	0.91 (0.75)	<0.001[a]
IL12p70	0.46 (0.72)	0.50 (0.70)	0.184	0.40 (0.52)	0.39 (0.55)	0.167
IL1β	−0.77 (0.75)	−0.84 (0.73)	0.253	−0.49 (0.64)	−0.58 (0.72)	0.265
IL2	−0.15 (0.55)	−0.27 (0.59)	0.013	0.02 (50)	−0.03 (0.57)	0.677
IL6	0.43 (0.45)	0.06 (0.59)	<0.001[a]	0.57 (0.52)	0.30 (0.54)	0.002
IL8	0.76 (0.20)	0.72 (0.24)	0.068	0.76 (0.18)	0.81 (0.27)	0.178
TNFα	0.90 (0.18)	0.84 (0.19)	0.012	0.97 (0.37)	0.97 (0.32)	0.752

Comparisons of C2D1-versus-BL for each cytokine within each treatment arm were done using the Wilcoxon rank sum test. Using testwise *P* value 0.05 and a Bonferroni adjustment for multiple testing, with 34 tests, a *P* value <0.00147 implies significant change for that cytokine in that treatment arm.

[a]Significant *P* values.

bFGF, basic fibroblast growth factor; BL, baseline; C2D1, cycle 2 day 1; GM-CSF, granulocyte macrophage-colony stimulating factor; hMMP9, human matrix metalloproteinase; IFNγ, interferon gamma; IL, interleukin; PIGF, placental growth factor; sVEGFR, soluble vascular endothelial growth factor receptor-2; TGFβ, transforming growth factor beta; TNFα, tumor necrosis factor alpha.

VEGF, and sVEGFR1 in the docetaxel-imatinib arm compared to the docetaxel-placebo arm, on average. The largest individual quantitative difference in cytokines between the arms was the decline in soluble c-kit in the docetaxel-imatinib arm.

TABLE 2. MEANS AND STANDARD DEVIATIONS (IN PARENTHESES) OF CHANGE FROM BASELINE TO COURSE 2 DAY 1 OF CHEMOTHERAPY FOR EACH CYTOKINE VARIABLE, WITHIN EACH TREATMENT ARM, COMPARED BETWEEN ARMS USING THE WILCOXON RANK SUM TEST

Cytokines	*Docetaxel + placebo*	*Docetaxel + imatinib*	*P*
TGFβ	0.07 (0.23)	−0.03 (0.22)	0.020
bFGF	0.01 (0.28)	0.03 (0.28)	0.847
PIGF	0.12 (0.14)	−0.08 (0.14)	<0.0001[a]
sVEGFR1	0.07 (0.12)	0.04 (0.24)	0.001[a]
VEGF	0.04 (0.13)	−0.06 (0.14)	<0.0001[a]
c-kit	<0.01 (0.08)	−0.14 (0.12)	<0.0001[a]
sVEGFR2	0.01 (0.07)	−0.03 (0.08)	0.017
hMMP9	0.04 (0.25)	−0.08 (0.26)	0.049
GM-CSF	−0.04 (0.99)	−0.08 (0.99)	0.509
IFNγ	−0.20 (0.94)	0.11 (1.24)	0.099
IL10	0.19 (0.51)	0.32 (0.52)	0.137
IL12p70	0.04 (0.22)	−0.01 (0.70)	0.075
IL1β	−0.09 (0.94)	−0.06 (1.07)	0.913
IL2	−0.14 (0.66)	0.01 (0.50)	0.095
IL6	−0.39 (0.49)	−0.27 (0.48)	0.278
IL8	−0.05 (0.20)	0.09 (0.46)	0.053
TNFα	−0.06 (0.18)	0.02 (0.23)	0.042

Using testwise *P* value 0.05 and a Bonferroni adjustment for multiple testing, with 17 tests, a *P* value <0.00294 implies significant change for that cytokine in that treatment arm.

[a]Significant *P* values.

The fitted piecewise linear regression models are summarized in Table 3. For each cytokine, the test of $(b_{0,DP}, b_{1,DP})$ $(b_{0,DI}, b_{1,DI})$ between the 2 treatment groups was performed using an *F* statistic with (2, 84) degrees of freedom. The results indicate that, among the 17 cytokines, the kinetics of 2 specific angiogenic cytokines, PIGF and soluble c-kit, differed significantly between the 2 treatment arms in terms of relationship to *in vivo* p-PDGFR dynamics, as summarized by Pr(Decr). These 2 cytokines were previously identified as among the 4 cytokines decreasing in the docetaxel–imatinib arm compared to the docetaxel–placebo arm (Table 2).

A total of 17 Bayesian log-normal regression models for PFS were fit, one for each cytokine. Because it would be far too cumbersome to tabulate all 17 fitted models, we present only the estimated effects of the C2D1-versus-BL cytokine changes, within each treatment arm, on PFS time. These are the parameters denoted above by β_8 and β_9 in the model linear component. Because parameters are random quantities under a Bayesian model, each parameter has a posterior distribution under the fitted model. For each combination of cytokine and treatment arm, Fig. 1 summarizes the posterior distribution of the parameter in terms of a 95% credible interval. This interval is represented by a vertical line running from the 2.5th percentile up to the 97.5th percentile of the effect's posterior distribution, with the posterior mean represented by an open circle for the DI arm and by a filled circle for the DP arm. Thus, each vertical line summarizes the middle 95% of the effect's posterior distribution. Under the Bayesian model, a line having lower limit near or above the horizontal line at 0 corresponds to a significant increase in PFS as a function of the C2D1-versus-BL cytokine change. For example, a line for β_8 having lower limit 0 would correspond to posterior probability $\Pr(\beta_8 > 0 \mid \text{data}) = 0.975$.

TABLE 3. SUMMARIES OF 17 FITTED REGRESSION MODELS, ONE FOR EACH CYTOKINE

Cytokine	Parameter	Docetaxel + placebo		Docetaxel + imatinib		Test for homogeneity between treatment groups
		Estimate	SE	Estimate	SE	P value
TGFβ						0.013
	Intercept	0.024	0.034	−0.061	0.041	
	Slope	1.825	0.661	0.555	0.379	
bFGF						0.431
	Intercept	−0.038	0.044	−0.008	0.053	
	Slope	1.826	0.858	0.504	0.492	
PlGF						<0.001[a]
	Intercept	0.131	0.023	−0.084	0.027	
	Slope	−0.336	0.442	0.037	0.253	
sVEGFR1						0.772
	Intercept	0.070	0.030	0.052	0.036	
	Slope	0.036	0.585	−0.228	0.335	
VEGF						0.004
	Intercept	0.032	0.022	−0.067	0.026	
	Slope	0.321	0.421	0.114	0.241	
c-kit						<0.001[a]
	Intercept	0.005	0.017	−0.139	0.020	
	Slope	−0.046	0.321	−0.005	0.184	
sVEGFR2						0.157
	Intercept	0.01	0.012	−0.018	0.015	
	Slope	−0.01	0.235	−0.16	0.135	
hMMP9						0.111
	Intercept	0.041	0.041	−0.095	0.05	
	Slope	−0.097	0.797	0.255	0.457	
GM-CSF						0.122
	Intercept	−0.160	0.159	0.073	0.190	
	Slope	5.201	3.057	−2.396	1.752	
IFNγ						0.630
	Intercept	−0.265	0.178	0.010	0.212	
	Slope	2.894	3.422	1.531	1.962	
IL10						0.246
	Intercept	0.245	0.083	0.358	0.100	
	Slope	−2.28	1.606	−0.552	0.921	
IL12p70						0.474
	Intercept	0.031	0.081	0.111	0.097	
	Slope	0.505	1.558	−1.782	0.893	
IL1β						0.922
	Intercept	−0.112	0.164	−0.034	0.195	
	Slope	0.986	3.148	−0.463	1.805	
IL2						0.475
	Intercept	−0.117	0.097	0.020	0.116	
	Slope	−0.865	1.865	−0.097	1.069	
IL6						0.169
	Intercept	−0.447	0.078	−0.236	0.093	
	Slope	2.393	1.499	−0.464	0.860	
IL8						0.156
	Intercept	−0.062	0.056	0.114	0.067	
	Slope	0.638	1.077	−0.36	0.618	
TNFα						0.129
	Intercept	−0.071	0.033	0.037	0.040	
	Slope	0.348	0.632	−0.227	0.362	

In each model, the change in cytokine value from BL to C2D1 is a piecewise linear function of the estimated Pr(Decr) for p-PDGFR, with different parameters for the 2 treatment groups, where Pr(Decr) is the estimated probability that p-PDGFR decreased from BL to C2D1. For each fitted model, the test for identical intercept and slope parameters in the treatment groups, "homogeneity," is based on an *F*-statistic with (2, 84) degrees of freedom. Using testwise *P* value 0.05 and a Bonferroni adjustment for multiple testing, with 17 tests, a *P* value <0.00294 implies significant heterogeneity between treatment groups, implying different p-PDGFR dynamics with versus without imatinib for that cytokine.

[a]Significant *P* values.

PDGFR, platelet-derived growth factor and its receptor; SE, standard error.

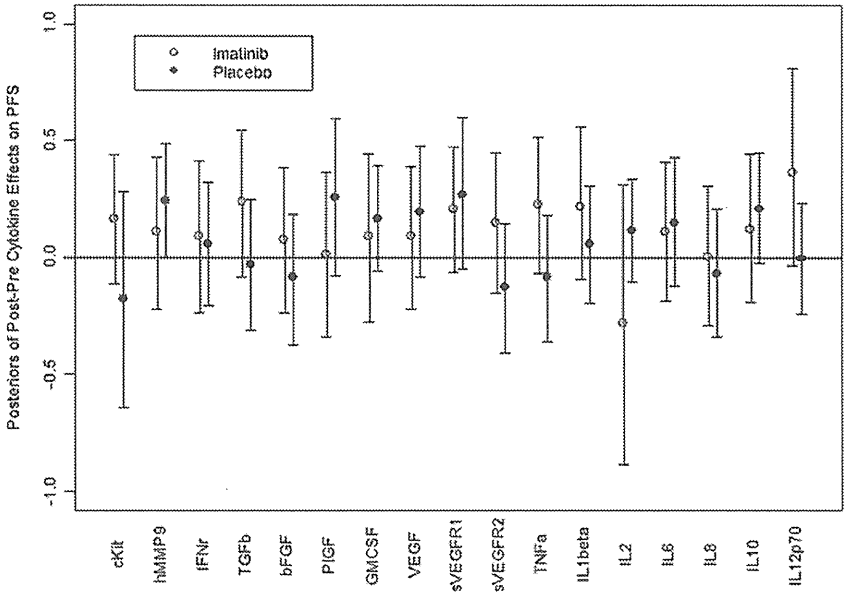

FIG. 1. Estimated posterior effect of each cycle 2 day 1-to-baseline cytokine change on progression-free survival (PFS) the baseline to cycle 2 day 1 change on PFS time for each cytokine within each treatment arm. Each effect was estimated under a Bayesian log-normal regression model, also accounting for the effects of Hb, change in prostate-specific antigen, and change in p-platelet-derived growth factor and its receptor. The posterior distribution of the parameter quantifying the effect of the in terms of a 95% credible interval. This interval is represented by a vertical line running from the 2.5th percentile to the 97.5th percentile of the effect's posterior distribution, with the posterior mean represented by an *open circle* for the docetaxel+imatinib arm and a *filled circle* for the docetaxel+placebo arm.

This would say that, given the observed data, the posterior probability that the effect of the cytokine's change on PFS is positive equals 0.975, a nominally significant effect. A vertical line with mean at 0 would correspond approximately to posterior probability $\Pr(\beta_8 > 0 \mid \text{data}) = 0.50$, interpreted as the cytokine change having no effect on PFS. Figure 1 shows that, in the DP arm, human MMP9 (hMMP9) had a significant effect, whereas nearly significant effects on PFS were seen for soluble VEGFR1 and IL-10. In the DI arm, a nearly significant effect on PFS was seen for IL-12p70.

Discussion

In this study, the kinetics of 17 angiogenic and inflammatory cytokines in men with metastatic castration-resistant prostate cancer receiving docetaxel with or without the c-kit/abl/PDGFR inhibitor imatinib mesylate were examined. Post-treatment cytokines are significantly modified compared to BL in both treatment arms (Table 1), and several differences vary significantly between both treatment arms (Table 2). Our prior observations had indicated that the status of p-PDGFR activation in peripheral blood leucocytes after docetaxel chemotherapy for castration-resistant prostate cancer associated with PFS and OS (Mathew and others 2008). We then studied the differences in cytokine kinetics between the 2 treatment arms when specifically partitioned by post-treatment *in vivo* p-PDGFR dynamics in peripheral blood leucocytes (Table 3). We find that among these 17 cytokines, PIGF and soluble c-kit dynamics specifically comprise the cytokine signature of imatinib effect after docetaxel chemotherapy.

Decline in soluble c-kit after imatinib therapy has been previously reported in gastrointestinal stromal tumors and has been proposed as a predictive factor for favorable outcome in that disease state (Bono and others 2004, DePrimo and others 2009). In this study, soluble c-kit decline in the imatinib-containing arm was the largest quantitative cytokine difference between the 2 arms. Along with PIGF kinetics, soluble c-kit post-treatment differences retained strong statistical significance when partitioned by p-PDGFR dynamics in peripheral blood leucocytes. These observations may be concordant with the mechanism of action of imatinib as a PDGFR and c-kit inhibitor.

Surprisingly however, in the imatinib arm, increases in soluble c-kit rather than decreases trended toward a favorable PFS profile (Fig. 1) and similarly larger post-treatment values of PIGF and VEGF after docetaxel-alone therapy trended toward an improved PFS. Together, these trends suggest that the cytokine profiles associated with imatinib (c-kit, PIGF, and, to a lesser extent, VEGF declines) compare unfavorably when compared to those generated by docetaxel alone. These findings are also compatible with our previous observations that decreased activation of p-PDGFR in peripheral blood leucocytes after imatinib exposure associated with shorter PFS times (Mathew and others 2008). With the exception of hMMP9 kinetics after docetaxel therapy alone, multivariate analysis of individual cytokine profiles did not yield an independent predictor of outcome. It is conceivable that, with larger numbers of patients, a composite picture of a favorable cytokine signature potentially linked to an *in vivo* mechanism of action of docetaxel may emerge through such cytokine profiling studies.

Declines in the angiogenic cytokines, PIGF, and VEGF after imatinib therapy have not been reported previously. The altered dynamics of these cytokines together with those previously reported with PDGF (Mathew and others 2008) comprise a candidate cytokine signature of imatinib effect in prostate cancer and bone metastases after docetaxel chemotherapy. Formal mechanistic studies will be required to identify the putative link between the regulation of plasma PIGF and VEGF levels and imatinib therapy. It is conceivable that kinetics of these markers may have predictive value in other disease states, hematological and solid neoplasia, in which imatinib has been established as standard therapy, as these circulating cytokines may not be tumor specific.

Before this report, there have been few studies that demonstrate the profile of changes and/or the predictive value of inflammatory and angiogenic cytokine dynamics after docetaxel therapy in prostate cancer. The wide range of

nonhematological toxicities observed with docetaxel, such as peripheral edema or pleural effusions that reflect vascular effects, or fatigue and pneumonitis that reflect proinflammatory effects, are likely to be reflected in plasma cytokine dynamics after treatment. In 2 prior studies, declines in plasma IL6 associated with PSA-declines after docetaxel were reported; however, associations with PFS or OS were not assessed (Domingo-Domenech and others 2006; Ignatoski and others 2009). Our observations do not support a significant association of IL6 decline after docetaxel with PFS (Fig. 1). While significant increases in PIGF and sVEGFR1 and significant decreases in IL6 were observed after docetaxel therapy (Table 1), only an increase in hMMP9 associated with improved PFS (Fig. 1). Elevated hMMP9 expression in prostate cancer has been associated with improved disease-free and OS after prostatectomy for localized prostate cancer (Boxler and others 2010), but a link of plasma MMP9 dynamics with docetaxel efficacy has not been described to our knowledge. These findings suggest the potential predictive value of a cytokine dynamic signature after chemotherapy for prostate cancer, for which larger prospective studies will be required for validation.

Acknowledgments

The authors acknowledge the assistance of Erin Horne and Sherryl Smith (Department of Genitourinary Medical Oncology) for research and administrative support and the M.D. Anderson Cancer Center Immune Monitoring Core Laboratory (IMCL) for assistance with the immunological assays. The IMCL is funded by the M.D. Anderson Cancer Center Support Grant (NCI # CA16672). P.F.T.'s research was partially supported by NCI grant RO1-CA-83932. The authors thank two referees for their detailed and constructive comments.

Author Disclosure Statement

P.M. is on the Speaker Bureau of Sanofi-Aventis. No other disclosures.

References

Bono P, Krause A, von Mehren M, and others. 2004. Serum KIT and KIT ligand levels in patients with gastrointestinal stromal tumors treated with imatinib. Blood 103:2939–2935.

Boxler S, Djonov V, Kessler TM and others. 2010. Matrix metalloproteinases and angiogenic factors: predictors of survival after radical prostatectomy for clinically organ-confined prostate cancer? Am J Pathol 177:2216–2224.

DePrimo SE, Huang X, Blackstein M, Garrett CR, Harmon CS, and others. 2009. Circulating levels of Soluble KIT serve as a biomarker for clinical outcome in gastrointestinal stromal tumor patients receiving sunitinib following imatinib failure. Clin Cancer Res 15:5869–5877.

Domingo-Domenech J, Oliva C, Rovira A and others. 2006. Interleukin-6, a nuclear factor-kB target, predicts resistance to docetaxel in hormone-independent prostate cancer and nuclear factor-kB inhibition by PS-1145 enhances docetaxel antitumor activity. Clin Cancer Res 12:5578–5586.

Hollander M, Wolfe DA. 1979. Introduction to the theory of nonparametric statistics. New York: John Wiley.

Ignatoski KMW, Friedman J, Escara-Wilke J, and others. 2009. Change in markers of bone metabolism with chemotherapy for advanced prostate cancer: interleukin-6 response is a potential early indicator of response to therapy. J Interferon Cytokine Res 29:105–111.

Kim SJ, Uehara H, Yazici S, and others. 2006. Targeting platelet-derived growth factor receptor on endothelial cells of multidrug-resistant prostate cancer. J Natl Cancer Inst 98:783–793.

Mathew P, Thall P, Bucana CD, and others. 2007. Platelet-derived growth factor receptor inhibition and chemotherapy for castration-resistant prostate cancer with bone metastases. Clin Cancer Res 13:5816–5824.

Mathew P, Thall PF, Wen S, and others. 2008. Dynamic change in phosphorylated platelet-derived growth factor receptor in peripheral blood leucocytes following docetaxel therapy predicts progression-free and overall survival in prostate cancer. Br J Cancer 99:1426–1432.

Morita S, Thall PF, Bekele BN, Mathew P. 2010. A Bayesian hierarchical mixture model for platelet derived growth factor receptor phosphorylation to improve estimation of progression-free survival in prostate cancer. J R Stat Soc C 59:19–34.

Snedecor GW, Cochran WG. 1980. Statistical methods, 7th ed. Ames: Iowa State University Press.

Uehara H, Kim SJ, Karashima T, and others. 2003. Effects of blocking platelet-derived growth factor-receptor signaling in a mouse model of experimental prostate cancer bone metastases. J Natl Cancer Inst 95:458–570.

Address correspondence to:
Dr. Paul Mathew
Department of Hematology–Oncology
Tufts Medical Center
800 Washington St., # 245
Boston, MA 02111

E-mail: pmathew@tuftsmedicalcenter.org

Received 17 November 2010/Accepted 17 January 2011